

Intensification of the Southern Hemisphere summertime subtropical anticyclones in a warming climate

Wenhong Li,¹ Laifang Li,¹ Mingfang Ting,² Yi Deng,³ Yochanan Kushnir,² Yimin Liu,⁴ Yi Lu,³ Chunzai Wang,⁵ and Pengfei Zhang^{4,6}

Received 26 September 2013; revised 11 November 2013; accepted 12 November 2013; published 26 November 2013.

[1] The Southern Hemisphere subtropical anticyclones (SAs) are important features of the Earth's climate. A broad consensus among Coupled Model Intercomparison Project phase 3 and phase 5 climate models suggests an intensification of summer SAs over SH oceans in association with the increase in greenhouse gas concentrations in the atmosphere. Diagnostic and modeling analyses conducted here demonstrate that the strengthening of the SAs is primarily caused by enhanced diabatic heating over continents and cooling over oceans in austral summer. This enhancement of Southern Hemisphere near-surface SAs identified here together with the enhancement of their Northern Hemisphere counterparts as suggested by Li et al. (2012) indicates increasingly important roles played by SAs in modulating weather and climate on regional and global scales. **Citation:** Li, W., L. Li, M. Ting, Y. Deng, Y. Kushnir, Y. Liu, Y. Lu, C. Wang, and P. Zhang (2013), Intensification of the Southern Hemisphere summertime subtropical anticyclones in a warming climate, *Geophys. Res. Lett.*, 40, 5959–5964, doi:10.1002/2013GL058124.

1. Introduction

[2] Connecting midlatitude westerlies with tropical easterlies, Southern Hemisphere subtropical anticyclones (SAs) are important elements of the summertime atmospheric circulation [Wu et al., 2009; Miyasaka and Nakamura, 2010; Lee et al., 2013]. In austral summer, SAs are closely related to the seasonal variation of moisture transport, precipitation [Lenters and Cook, 1999; Taschetto and Wainer, 2008], and tropical cyclone movement [Bannister et al., 1997]. The near-surface maritime anticyclonic systems could also strongly influence marine boundary layer (MBL) clouds

and associated radiation budget [Garreaud et al., 2001; Wang et al., 2004] through their interaction with sea surface temperatures (SSTs) and the clouds [Klein and Hartmann, 1993; Rahn and Garreaud, 2010]. Thus, intensity changes of the SAs have major implications for climate change at both regional and global scales.

[3] Recent studies found that both Northern Hemisphere SAs have intensified in boreal summer [Zhou et al., 2009; Li et al., 2011, 2012]. The enhancement of the Northern Hemisphere SAs is primarily attributed to an increase in the land-sea thermal contrast during boreal summer in a warming climate [Li et al., 2012]. However, whether the intensity of the summertime SAs over Southern Hemisphere oceans is also changing has yet to be investigated. Climatologically, the Southern Hemisphere SAs share similar dynamics with their Northern Hemisphere counterparts [Wu et al., 2009; Miyasaka and Nakamura, 2010], i.e., they are forced by longwave (LO) radiative cooling over eastern oceans, sensible heating (SH) and condensational (CO) heating over western and eastern continents, respectively. Such heating patterns largely determine the strength of the SAs [Wu and Liu, 2003; Miyasaka and Nakamura, 2005; Wu et al., 2009]. It is unclear whether the physical mechanisms associated with the intensity changes of the SAs in Southern Hemisphere in a warming climate bear similarities with those responsible for the observed changes in their Northern Hemisphere counterparts. Understanding the intensity changes in the Southern Hemisphere SAs and the possible causes can help improve prediction of regional weather and climate.

[4] This work investigates the intensity change of the low-level summertime SAs over the Indian Ocean (IOSA), the South Pacific (SPSA), and the South Atlantic (SASA) through data diagnosis and numerical modeling. Possible mechanisms responsible for the intensity change of the Southern Hemisphere SAs are investigated.

2. Data and Methods

[5] Data used in this study consist of atmospheric circulation field from the 40 year European Centre for Medium-Range Weather Forecasts (ECMWF) Re-Analysis (ERA-40) from 1958 to 2002 [Uppala et al., 2005] and from both the Coupled Model Intercomparison Project phase 3 (CMIP3) and phase 5 (CMIP5) of the Intergovernmental Panel on Climate Change Fourth and Fifth Assessment Reports, respectively. An idealized general circulation model (IGCM) is adopted to further examine the processes responsible for the intensity change of the Southern Hemisphere SAs in a warming climate (see supporting information for more details).

Additional supporting information may be found in the online version of this article.

¹Earth and Ocean Sciences, Nicholas School of the Environment, Duke University, Durham, North Carolina, USA.

²Lamont-Doherty Earth Observatory, Earth Institute, Columbia University, Palisades, New York, USA.

³Earth and Atmospheric Sciences, Georgia Institute of Technology, Atlanta, Georgia, USA.

⁴State Key Laboratory of Numerical Modeling for Atmospheric Sciences and Geophysical Fluid Dynamics, Institute of Atmospheric Physics, Chinese Academy of Sciences, Beijing, China.

⁵NOAA Atlantic Oceanographic and Meteorological Laboratory, Miami, Florida, USA.

⁶University of Chinese Academy of Sciences, Beijing, China.

Corresponding author: W. Li, Earth and Ocean Sciences, Nicholas School of the Environment, Duke University, PO Box 90227, 321C Old Chem Bldg., Durham, NC 27708-0227, USA. (wenhong.li@duke.edu)

©2013. American Geophysical Union. All Rights Reserved.
0094-8276/13/10.1002/2013GL058124

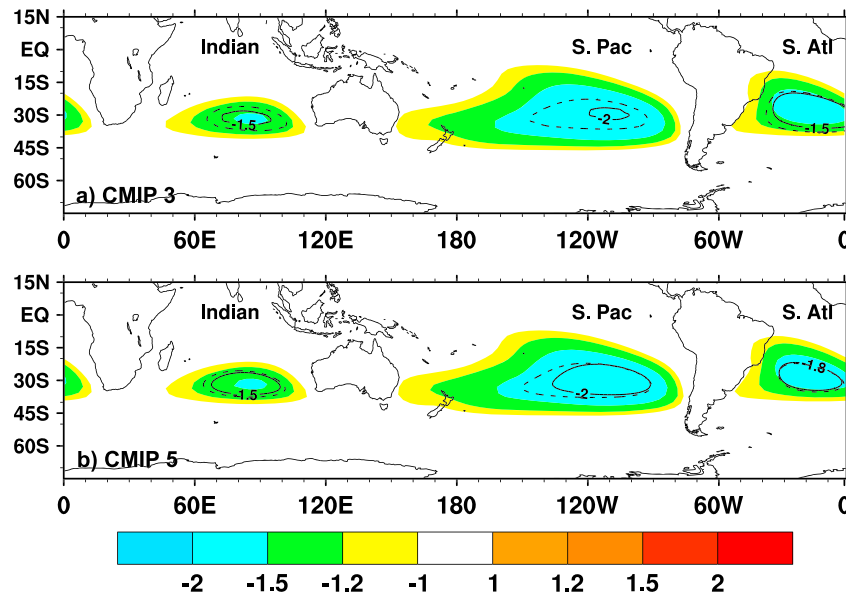


Figure 1. Southern Hemisphere SAs climatology during December to February using 925 hPa stream function (unit: $10^7 \text{ m}^2 \text{ s}^{-2}$) of the ERA-40 (shaded) and (top) CMIP3 and (bottom) CMIP5 MME mean (contour). The centers' stream function of the subtropical anticyclones in the South Atlantic, South Pacific, and Indian Ocean are drawn, respectively, in the 20th (1950–1999, solid contours) and the 21st century (2050–2099, dashed contours) using the CMIP3 and CMIP5 models' ensemble mean.

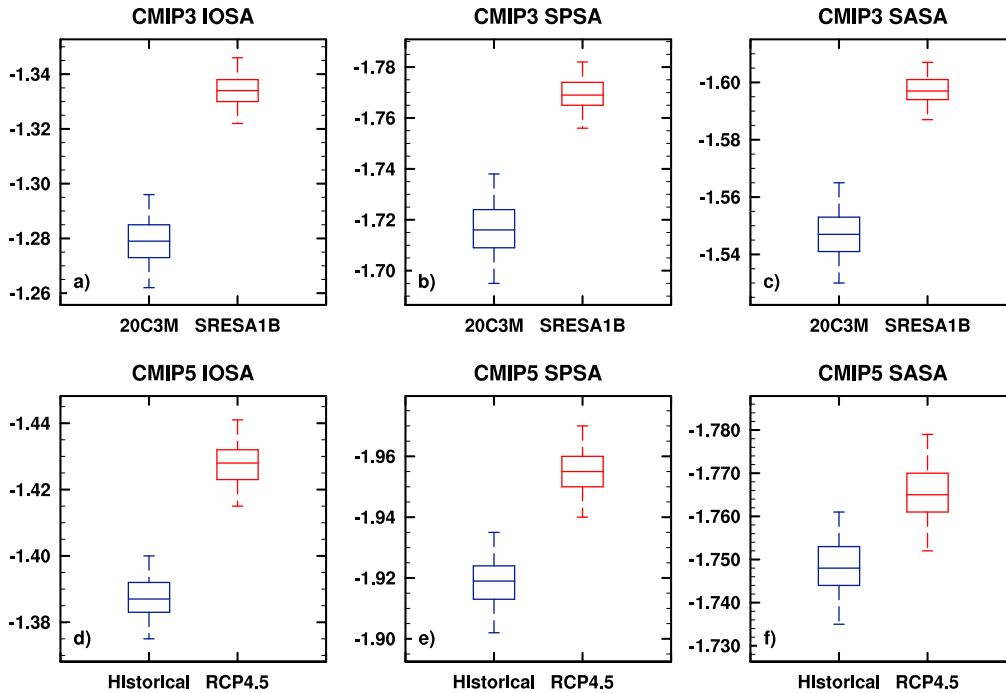


Figure 2. Projected changes in the domain-averaged 925 hPa stream function for the Southern Hemisphere SAs in the (a) Indian Ocean (IOSA), (b) South Pacific (SPSA), and (c) South Atlantic (SASA) Oceans from the 20th (1950–1999) to the 21st century (2050–2099) using all (top) CMIP3 and (bottom) CMIP5 models. The middle lines represent the 50th percentile or median prediction of all the models. The top and bottom of the box represent the 75% and 25% percentiles, respectively. The top and bottom “whiskers” plot the 2.5% and 97.5% percentiles (unit: $10^7 \text{ m}^2 \text{ s}^{-2}$).

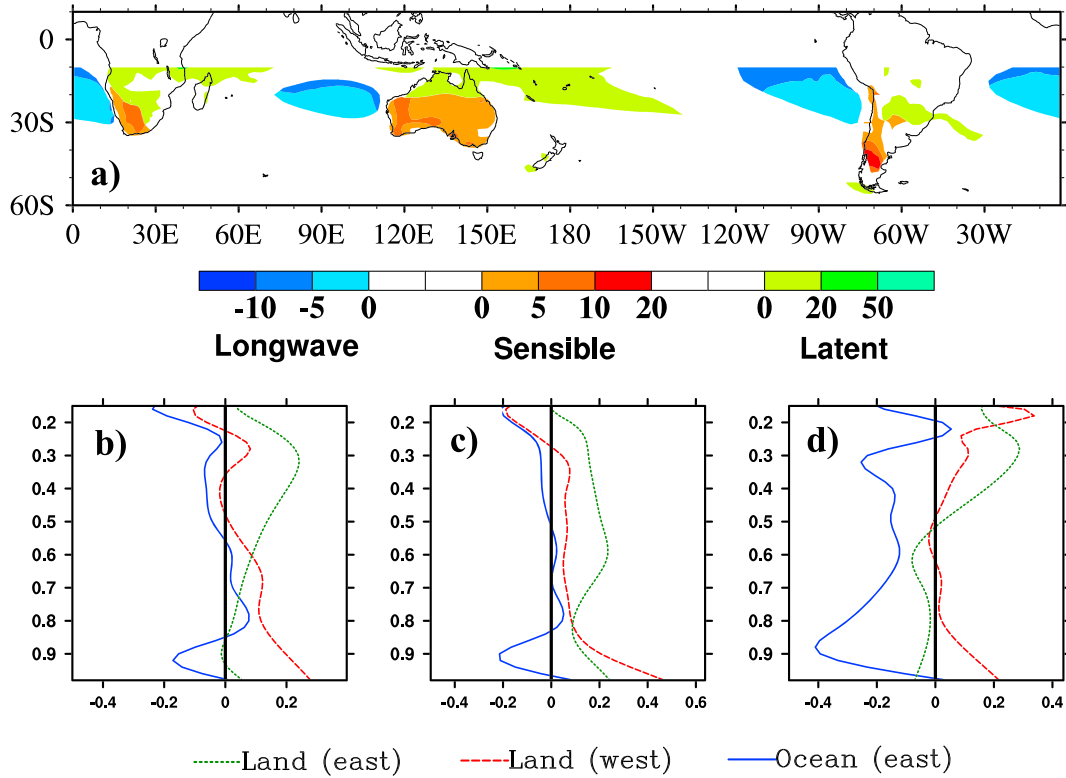


Figure 3. (a) Changes in column-integrated dominant heating components, i.e., longwave radiative cooling (blue), sensible heating (red), and condensational heating (green), respectively, obtained from CMIP3 models; and changes of MME mean total diabatic heating at different levels over subtropical (b) Atlantic-South Africa-Indian Ocean, (c) Indian Ocean-Australia-Pacific, and (d) Pacific-South America-Atlantic regions similar to *Wu and Liu* [2003] between the 21st (2050–2099) and 20th century (1950–1999). The y axis in Figures 3b–3d: the σ -coordinate. Unit in Figure 3a: W m^{-2} . Unit in Figures 3b–3d: K d^{-1} .

3. Results

3.1. Intensity Changes of the Southern Hemispheric SAs in Current and Future Climates

[6] Historically, there are two methods to define the intensity of SAs: the maximum stream function and the domain-averaged stream function over the climatological SA regions [*Liu and Wu*, 2004; *Liu et al.*, 2007]. The domains used in the study are 40°S – 20°S and 140°W – 80°W for the SPSA, 35°S – 25°S and 45°W – 10°W for the SASA, and 35°S – 20°S and 60°E – 100°E for the IOSA, respectively. The two methods show similar results in the SAs' intensity change.

[7] Summertime climatological maritime anticyclonic systems from CMIP3 and CMIP5 models' simulation are first compared with those in ERA-40 that illustrate weaker low-level anticyclonic circulation over South Atlantic and Indian Ocean than that over South Pacific (Figure 1). During the period 1958–2002, the ERA-40 shows significant strengthening of all three SAs: the average stream function increased by $-1.1 \times 10^5 \text{ m}^2 \text{ s}^{-2}/\text{decade}$, $-6.9 \times 10^5 \text{ m}^2 \text{ s}^{-2}/\text{decade}$, and $-3.1 \times 10^5 \text{ m}^2 \text{ s}^{-2}/\text{decade}$ for the SPSA, the SASA, and the IOSA, respectively, and the trends of intensification are significant, with 95% confidence (the Mann-Kendall test).

[8] Compared to ERA-40, CMIP3 (CMIP5) model reasonably captures the shapes of the three maritime anticyclones in the twentieth century (1950–1999) (Figure 1a), but the intensities of the anticyclones are overestimated in CMIP3 and CMIP5 models. Specifically, multimodel ensemble (MME) mean intensity of the IOSA, the SPSA, and the SASA

simulated by CMIP3 (CMIP5) model is systematically stronger by 6.6% (12.4%), 3.6% (13.7%), and 6.8% (19.9%), respectively.

[9] In the future, CMIP3 (CMIP5) model projects consistent expansion and center intensification for all three SAs in austral summer (Figure 1): The anticyclones tend to expand more zonally and westward, especially for the SPSA. Domain-averaged intensity of the SPSA simulated by the CMIP3 (CMIP5) model increases from -1.716×10^7 (-1.919×10^7) $\text{m}^2 \text{ s}^{-2}$ (95% confidence interval based on t test: -1.695×10^7 and $-1.74 \times 10^7 \text{ m}^2 \text{ s}^{-2}$ for CMIP3 and -1.902×10^7 and $-1.935 \times 10^7 \text{ m}^2 \text{ s}^{-2}$ for CMIP5) in the twentieth century (1950–1999) to $-1.77 \times 10^7 \text{ m}^2 \text{ s}^{-2}$ (-1.955×10^7) $\text{m}^2 \text{ s}^{-2}$ (95% confidence interval: -1.755×10^7 and $-1.783 \times 10^7 \text{ m}^2 \text{ s}^{-2}$ for CMIP3 and -1.94×10^7 and $-1.97 \times 10^7 \text{ m}^2 \text{ s}^{-2}$ for CMIP5) in the 21st century (2050–2099; Figures 2b and 2e). The difference between the SPSA intensity in the 21st and the 20th century simulations by CMIP3 and CMIP5 models are at 0.0001 significance level (χ^2 test).

[10] Similar results are also found for the SASA and the IOSA using CMIP3 (CMIP5) models: domain-averaged SASA intensity is enhanced from $-1.547 \times 10^7 \text{ m}^2 \text{ s}^{-2}$ (-1.748×10^7) $\text{m}^2 \text{ s}^{-2}$ in the twentieth century simulation to $-1.597 \times 10^7 \text{ m}^2 \text{ s}^{-2}$ ($-1.765 \times 10^7 \text{ m}^2 \text{ s}^{-2}$) in the 21st century simulation, and the MME mean intensity of the IOSA is enhanced from $-1.277 \times 10^7 \text{ m}^2 \text{ s}^{-2}$ ($-1.386 \times 10^7 \text{ m}^2 \text{ s}^{-2}$) during the period 1950–1999 to -1.335×10^7 ($-1.428 \times 10^7 \text{ m}^2 \text{ s}^{-2}$) $\text{m}^2 \text{ s}^{-2}$ during the period 2050–2099. The intensity

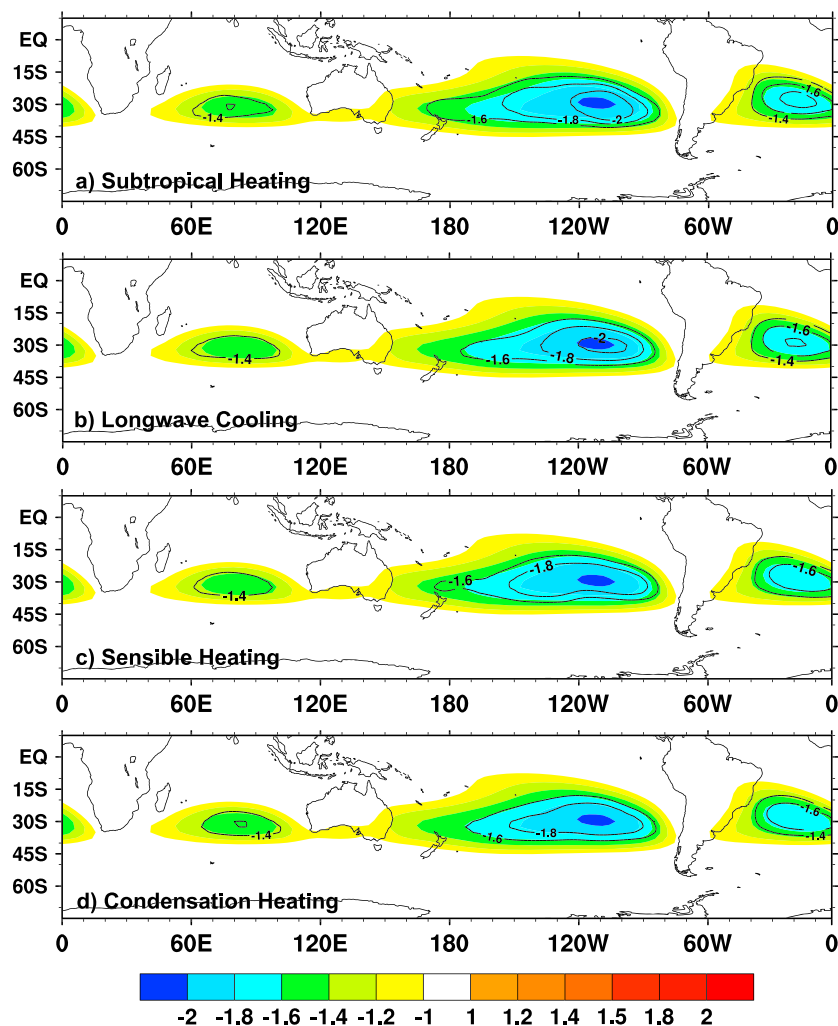


Figure 4. Southern Hemisphere SAs simulated by the IGCM (contour) with changes in total diabatic heating over (a) subtropics (15°S–45°S), (b) longwave cooling dominant area, (c) sensible heating dominant area, and (d) condensational heating dominant area, compared to their twentieth century climatology (shaded) as indicated by 925 hPa stream function. Unit: $10^7 \text{ m}^2 \text{ s}^{-2}$.

differences of the SASA and the IOSA between the 20th and the 21st century simulations are significant at 0.01 level (χ^2 test).

[11] In addition to the intensification of the anticyclonic circulations, the central areas of the anticyclones expand by about 500% (60%), 60% (30%), and 200% (100%) for the SPSA, the SASA, and the IOSA in CMIP3 (CMIP5) models, respectively. Overall, CMIP3 and CMIP5 model simulations indicate a consistent intensification of the three maritime anticyclonic systems during austral summer over Southern Hemisphere in a greenhouse gasses (GHGs) increase scenario.

3.2. Physical Mechanism for the Southern Hemisphere SAs' Strengthening

[12] Climatologically, Southern Hemisphere near-surface SAs share similar dynamics to their Northern Hemisphere counterparts [Wu *et al.*, 2009; Miyasaka and Nakamura, 2010]. In the summer subtropics (15°S–45°S), the dominant diabatic heating is organized as follows: SH and CO heating over the western and eastern continents and LO cooling over eastern oceans, i.e., heat sources (sinks) over lands (oceans)

[Wu and Liu, 2003; Miyasaka and Nakamura, 2005; Wu *et al.*, 2009]. Corresponding to such heating patterns, atmospheric circulation in the subtropics is thus formed as anticyclonic (cyclonic) circulation over oceans and cyclonic (anticyclonic) circulation over continents in the lower (upper) troposphere [Wu and Liu, 2003; Miyasaka and Nakamura, 2005; Wu *et al.*, 2009]. We will examine whether this diabatic heating critical to the summertime SAs in Southern Hemisphere changes and how the changes of heating alter the intensity of the near-surface SAs from the 20th to the 21st century, when GHGs increase through the analyses of CMIP3 models and IGCM experiments.

[13] Figure 3a demonstrates the column-integrated dominant heating change from the period of 1950–1999 to 2050–2099. Increases of SH (CO) heating are mainly over western subtropical Africa, southern Australia, and western South America (central and eastern subtropical Africa, North Australian monsoon region, the south Pacific convergence zone, and central to eastern South America between 20°S and 30°S), and enhanced LO cooling is mainly over the eastern South Atlantic, eastern South Pacific, and South

Indian Ocean. Consistent with the changes in the dominant heating component, total diabatic heating increases (decreases) over continents (eastern oceans). Specifically, increased total heating over western continents is characterized by the maximum increase near the surface, and less changes with increasing altitude, suggesting that total diabatic heating change is dominated by SH heating change over the western continents (Figure 3c). Increased total heating over eastern continents from the 20th to 21st century are more obvious in the middle to upper troposphere, a prominent feature of CO heating (Figure 3b). LO cooling is also enhanced over eastern oceans (Figure 3d). Overall, the spatial pattern of diabatic heating enhancement from the 20th to 21st century (Figure 3) is similar to the heating climatology [Wu and Liu, 2003; Miyasaka and Nakamura, 2010] thus favors a stronger anticyclonic circulation over oceans, consistent with other studies [Seager et al., 2003; Liu et al., 2004; Nakamura et al., 2010].

[14] To verify the results from data analysis, we further perform simulations with an IGCM to study the impact of the heating changes discussed above on the intensity variations of the Southern Hemisphere SAs. Figure 4a compares the forced circulation field to the circulation in which only CMIP3 climatological planetary-scale flow is included in austral summer. Responding to the total diabatic heating change, the modeled intensity of the SPSA is enhanced, with maximum stream function changing from $-2.04 \times 10^7 \text{ m}^2 \text{ s}^{-2}$ to $-2.26 \times 10^7 \text{ m}^2 \text{ s}^{-2}$ and the anticyclone's central area (stronger than $-2.0 \times 10^7 \text{ m}^2 \text{ s}^{-2}$) expanding by about 375%. As we will show shortly, the intensification of the SPSA driven by the total diabatic heating changes (Figure 4a) is stronger than the sum of the modeled stream function responses to three individual heating changes (Figures 4b–4d), suggesting the existence of strong nonlinearity in the system. Similar to the SPSA, the intensities of the IOSA and SASA increase (Figure 4a), with a relatively uniform expansion for the SASA, more westward expansion for the IOSA (Figure 4a).

[15] We also investigate the changes of the SA intensities (Figures 4b–4d) associated with changes in SH heating over the western continents (Figures 3a and 3c), CO heating over eastern continents (Figures 3a and 3d), and LO cooling over eastern oceans (Figures 3a and 3b), separately. Figure 4c shows intensification and zonal expansion of the SPSA and IOSA responding to the increase of SH heating in the 21st century. The SASA shifts slightly eastward but no significant change of its intensity. Accompanying with the enhanced LO cooling over the eastern oceans, the three SAs all intensify (Figure 4b). The intensification is more apparent around the center of the SPSA and the SASA, and the former shifts eastward. The IOSA expands westward slightly (Figure 4b). Figure 4b suggests an important role of the LO cooling associated with MBL clouds over the eastern south Pacific and Atlantic in the SAs intensity. Note that the IGCM used here does not include the two-way coupling processes between the SAs and diabatic heating anomalies associated with local SSTs and MBL clouds variations; additional experiments with a fully coupled atmosphere-ocean model are needed to further confirm the findings here, which constitute our next research step. Corresponding to the changes of CO heating, the IOSA intensifies, especially at its center, while the SPSA expands westward slightly (Figure 4d), but the SASA does not change much. Figure 4 thus suggests that the intensification of the three southern hemisphere SAs is closely related with collectively diabatic heating changes from the 20th to the 21st century.

IGCM experiments further prove that the enhancement of the low-level subtropical anticyclonic circulations over Southern Hemisphere oceans largely results from the stronger diabatic heating over land and is associated with LO cooling over oceans during austral summer in the future.

4. Summary

[16] Using the ERA-40, 23 CMIP3 and 30 CMIP5 model outputs, and IGCM simulations, this study assesses current and future changes in the strength of the summertime near-surface SAs over Southern Hemisphere oceans. CMIP3 and CMIP5 models project an unambiguous intensification of the three SAs in austral summer when GHGs increase. CMIP3 and CMIP5 models and the IGCM experiments suggest that the projected strengthening of these SAs can be interpreted as a collective response to the enhanced warming over continents and cooling over oceans and also to the possible feedbacks between the SAs and the MBL clouds especially over the South Pacific and South Atlantic, which is consistent with the current understanding of the dynamical forcings of SAs [Liu et al., 2004; Miyasaka and Nakamura, 2005; Seager et al., 2003; Nakamura, 2012]. These results along with those from Li et al. [2012] demonstrate that intensification of summer SAs over oceans is a global phenomenon in the current and future climates. These results imply increasingly important roles played by global subtropical anticyclones in modulating regional and global weather and climate patterns as their intensities rise.

[17] **Acknowledgments.** We acknowledge the World Climate Research Programme's Working Group on Coupled Modelling, which is responsible for CMIP, and we thank the international modeling groups for producing and making available their model output. For CMIP, the U.S. Department of Energy's Program for Climate Model Diagnosis and Intercomparison provides coordinating support and led development of software infrastructure in partnership with the Global Organization for Earth System Science Portals. We also thank Guoxiong Wu and Gudrun Magnusdottir for helpful discussion, Cuihua Li for graphic help, and Ming Cai and an anonymous reviewer for insightful comments. This work is supported by the NSF AGS 1147608, NSF AGS 1147601, NSF ATM 07-39983, and NOAA grant NA10OAR4320137.

[18] The Editor thanks an anonymous reviewer and Tianjun Zhou for their assistance evaluating this manuscript.

References

- Bannister, A. J., M. A. Boothe, L. E. Carr, and R. L. Elsberry (1997), *Southern Hemisphere Application of the Systematic Approach to Tropical Cyclone Track Forecasting: Part I: Environmental Structure Characteristics*, Tech. Rep. NPS-MR-98-001, 96 p., Naval Postgraduate School, Monterey, CA.
- Garreaud, R. D., J. Rutllant, J. Quintana, J. Carrasco, and P. Minnis (2001), CIMAR-5: A snapshot of the lower troposphere over the subtropical southeast Pacific, *Bull. Am. Meteorol. Soc.*, 82, 2193–2207.
- Klein, S. A., and D. L. Hartmann (1993), The seasonal cycle of low stratiform clouds, *J. Clim.*, 6, 1587–1606.
- Lee, S.-K., C. R. Mechoso, C. Wang, and J. D. Neelin (2013), Interhemispheric influence of the northern summer monsoons on the southern subtropical anticyclones, *J. Clim.*, doi:10.1175/JCLI-D-13-00106.1, in press.
- Lenters, J. D., and K. H. Cook (1999), Summertime precipitation variability over South America: Role of the large-scale circulation, *Mon. Weather Rev.*, 127, 409–431.
- Li, W., L. Li, R. Fu, Y. Deng, and H. Wang (2011), Changes to the North Atlantic subtropical high and its role in the intensification of summer rainfall variability in the southeastern United States, *J. Clim.*, 24, 1499–1506.
- Li, W., L. Li, M. Ting, and Y. Liu (2012), Intensification of Northern Hemisphere subtropical highs in a warming climate, *Nat. Geosci.*, 5, 830–834.
- Liu, Y., and G. Wu (2004), Progress in the study on the formation of the summertime subtropical anticyclone, *Adv. Atmos. Sci.*, 21, 322–342.
- Liu, Y., G. Wu, and R. Ren (2004), Relationship between the subtropical anticyclone and diabatic heating, *J. Clim.*, 17, 682–698.

- Liu, Y., B. J. Hoskins, and M. Blackburn (2007), Impacts of the Tibetan Topography and heating on the summer flow over Asia, *Meteorol. Soc. Jpn.*, *85B*, 1–19.
- Miyasaka, T., and H. Nakamura (2005), Structure and formation mechanisms of the Northern Hemisphere summertime subtropical highs, *J. Clim.*, *18*, 5046–5065.
- Miyasaka, T., and H. Nakamura (2010), Structure and mechanisms of the Southern Hemisphere summertime subtropical anticyclones, *J. Clim.*, *23*, 2115–2130.
- Nakamura, H. (2012), Atmospheric science: Future oceans under pressure, *Nat. Geosci.*, *5*, 768–769.
- Nakamura, H., T. Miyasaka, Y. Kosaka, K. Takaya, and M. Honda (2010), Northern Hemisphere extratropical tropospheric planetary waves and their low-frequency variability: Their vertical structure and interaction with transient eddies and surface thermal contrasts, in *Climate Dynamics: Why Does Climate Vary?*, edited by D.-Z. Sun and F. Bryan, pp. 149–179, AGU, Washington, D. C., doi:10.1029/2008GM000789.
- Rahn, D. A., and R. Garreaud (2010), Marine boundary layer over the subtropical southeast Pacific during VOCALS-REx—Part 1: Mean structure and diurnal cycle, *Atmos. Chem. Phys.*, *10*, 4491–4506.
- Seager, R., R. Murtugudde, N. Naik, A. Clement, N. Gordon, and J. Miller (2003), Air-sea interaction and the seasonal cycle of the subtropical anticyclones, *J. Clim.*, *16*, 1948–1966.
- Taschetto, A. S., and I. Wainer (2008), The impact of the subtropical South Atlantic SST on South American precipitation, *Ann. Geophys.*, *26*, 3457–3476.
- Uppala, S. M., et al. (2005), The ERA-40 re-analysis, *Q. J. R. Meteorol. Soc.*, *131*, 2961–3012.
- Wang, Y., S.-P. Xie, H. Xu, and B. Wang (2004), Regional model simulations of marine boundary layer clouds over the southeast Pacific off South America. Part I: Control experiment, *Mon. Weather Rev.*, *132*, 274–296.
- Wu, G., and Y. Liu (2003), Summertime quadruplet heating pattern in the subtropics and the associated atmospheric circulation, *Geophys. Res. Lett.*, *30*(5), 1201, doi:10.1029/2002GL016209.
- Wu, G., Y. Liu, X. Zhu, W. Li, R. Ren, A. Duan, and X. Liang (2009), Multi-scale forcing and the formation of subtropical desert and monsoon, *Ann. Geophys. Germany*, *27*, 3631–3644.
- Zhou, T., et al. (2009), Why the western Pacific subtropical high has extended westward since the late 1970s, *J. Clim.*, *22*, 2199–2215.